

Low Levels of Sulphur Dioxide Contamination of Phosphine Spectra from
Venus' Atmosphere

Jane S. Greaves^{1,2}, Paul B. Rimmer^{3,4,5}, Anita M. S. Richards⁶, Janusz J. Petkowski⁷, William Bains^{2,7}, Sukrit Ranjan⁸, Sara Seager^{7,9,10}, David L. Clements¹¹, Clara Sousa Silva¹², Helen J. Fraser¹³

Abstract

New analysis is presented of the 1.1 mm wavelength absorption lines in Venus' atmosphere that suggested the presence of phosphine. We confirm that ALMA detected absorption at the PH₃ 1-0 wavelength in 2019, from an optimised spectrum covering half of the planetary disc. Sulphur dioxide line-contamination was then <10%, from modelling of a simultaneous ALMA spectrum of SO₂. We retrieve an SO₂ observation from the JCMT archive that was simultaneous within a few days of the PH₃ 1-0 spectrum obtained in June 2017, and demonstrate that contamination was also <10%. The contamination-subtracted ALMA and JCMT spectra (of 6-7 sigma confidence) are now consistent with similar levels of absorption. The variation is ~25% around -1.5 10⁻⁴ of the continuum, albeit not for identical planetary areas. This similarity suggests the abundance that can be attributed to phosphine in Venus' atmosphere was broadly similar in 2017 and 2019.

¹ Corresponding author Greavesj1@cardiff.ac.uk

² School of Physics & Astronomy, Cardiff University, 4 The Parade, Cardiff CF24 3AA, UK

³ Department of Earth Sciences, University of Cambridge, Downing Street, Cambridge CB2 3EQ, UK

⁴ Cavendish Astrophysics, University of Cambridge, JJ Thomson Avenue, Cambridge CB3 0HE, UK

⁵ MRC Laboratory of Molecular Biology, Francis Crick Ave, Trumpington, Cambridge CB2 0QH, UK

⁶ Jodrell Bank Centre for Astrophysics, Department of Physics and Astronomy, The University of Manchester, Manchester, UK

⁷ Department of Earth, Atmospheric, and Planetary Sciences, Massachusetts Institute of Technology, 77 Mass. Ave., Cambridge, MA, 02139, USA

⁸ Northwestern University, 1800 Sherman Avenue #8041, Evanston, IL 60201, USA

⁹ Department of Physics and Kavli Institute for Astrophysics and Space Research, Massachusetts Institute of Technology, 77 Mass. Ave., Cambridge, MA, 02139, USA

¹⁰ Dept. of Aeronautics and Astronautics, Massachusetts Institute of Technology, 77 Mass. Ave., Cambridge, MA, 02139, USA

¹¹ Department of Physics, Imperial College London, South Kensington Campus, London SW7 2AZ, UK

¹² Harvard-Smithsonian Center for Astrophysics, Observatory Building E, 60 Garden St, Cambridge, MA 02138, USA

¹³ School of Physical Sciences, The Open University, Walton Hall, Milton Keynes MK7 6AA, UK

1. INTRODUCTION

There is presently little concensus about the possible presence of phosphine, PH_3 , in Venus' atmosphere. This trace-gas would be very unexpected for an oxidised planet, but could come from unknown chemical routes (Bains et al. 2021), or even be a biological by-product, although ultra-dry/acidic cloud conditions would be uninhabitable by any known life (Seager et al. 2021, Hallsworth et al. 2021). In Greaves et al. (2020) we presented 1.1 mm-wavelength absorption features, seen by JCMT and ALMA independently, and interpreted as from PH_3 in Venus' atmosphere owing to close alignment with the 1-0 rotational-transition frequency. Mogul et al. (2021) then retrospectively attributed to phosphine a signal recorded by the Pioneer-Venus mass spectrometer LNMS, which sampled the clouds in 1978. All these signals were around 5-sigma confidence. Further searches for phosphine are currently very difficult - shorter-wavelength absorption only traces above-cloud layers (Trompet et al. 2021), and further in-situ sampling awaits new missions.

Critiques of the JCMT/ALMA results have posed three main questions: (1) are the 1.1 mm features robust? (2) could they be due to SO_2 absorption rather than PH_3 ? (3) do the line-widths observed suggest the absorbing gas is at high altitude, where PH_3 -presence would be problematic as it is rapidly destroyed by photo-chemical processes? Regarding (1), we presented (Greaves et al. 2021a,b) new data-processing addressing technical issues (Villanueva et al. 2021) and statistics on false-positives (Snellen et al. 2020; Thompson 2020). We now focus on (2), presenting new analysis to quantify the level of SO_2 contamination of the 1.1 mm features we attributed to PH_3 , in response to the critiques of Akins et al. (2021) and Lincowski et al. (2021). Addressing (3) requires new observations and better laboratory data, as inversion of line-shapes to altitude-profiles needs both high signal-to-noise spectra and a PH_3 - CO_2 broadening-coefficient that improves on current theoretical estimates.

The 1.1 mm data in-hand include: from JCMT, a spectrum observed over a week in June 2017, covering the whole planet, and from ALMA, a datacube from one morning in March 2019, where the planet was spatially resolved. In the latter, issues with spatial filtering (Villanueva et al. 2021, Akins et al. 2021, Greaves et al. 2021a) result in the limb being the best-sampled region.

2. DATA PROCESSING AND MODELLING

The original ALMA processing suffered from several issues in bandpass calibration and flux-scaling. The observations were non-optimal in calibration, being exploratory in high dynamic range for line:continuum. After the observatory (JAO) re-calibrated and re-released the data in late 2020, line-shapes were seen to be improved, but there were some caveats on recoverable area and line:continuum fidelity. In Greaves et al. (2021a), we omitted more noisy/ripply parts of the dataset (larger scales and north/south parts of the field), and applied simultaneously-observed continuum signals rather than a Venus model. Here we further maximise signal-to-noise ratio (S/N) and planetary area that is recoverable. Our optimisations beyond the JAO-released re-processing are the exclusion of antenna-baselines $<33\text{m}$ (hence angular scales $>30\%$ planetary-diameter) and application of low-order image-plane fits (6th-order for narrowband data including PH₃ 1-0, 3rd-order for wideband data covering a strong SO₂ transition). Full details were presented in Greaves et al. (2021a). The only further post-processing here is on the wideband-data which suffered particularly from spectral ripple. We found that these ripples are quasi-periodic on the frequency axis, and experimented with self-cancellation. Shifting the data by $\sim 150\text{ km/s}$ created a “model” line-free section of spectral baseline which could then be subtracted from the unshifted data. This procedure has partially cancelled the largest ripples.

The JCMT PH₃ spectra were acquired with bandwidth insufficient to cover any strong SO₂ transitions. However, we have now found nearly contemporaneous monitoring of SO₂ in the JCMT public archive. The JCMT’s HARP camera-spectrometer observed Venus twice in May 2017 and then on 6 June 2017 – just before the PH₃ observations on 9–16 June 2017. HARP observed at 346.6 GHz with a telescope beam of $\approx 14\text{ arcsec}$, while Venus’ diameter on 6 June 2017 was 23 arcsec. The planet was thus undersampled by the on-source receptor, but HARP receptors at 30 arcsec-offsets saw the planetary limb in the first sidelobe. We tested co-adding these offset line:continuum spectra with the planet-centre spectrum, with various weightings up to 50%, and found only up to $\sim 10\%$ changes in SO₂ line-depth. The planet-centre spectrum (best S/N) is thus adopted as representing net planetary SO₂. We downloaded the raw archival spectra (~ 30 min observations, at 0.98 MHz spectral resolution), created one-pixel datacubes with ‘makecube’ in SMURF, and corrected for Venus-Earth velocity-differences ($>10\text{ km/s}$) within SPLAT. The resulting SO₂ 19_{1,19}–18_{0,18} (346.65217 GHz) lines have high S/N but some spectral ripple is evident.

Here we model sulphur dioxide spectra using the simplified radiative-transfer code of Greaves et al. (2021a) – the implementation is described here in the Appendix, and a link is provided to example code. The advantage of this simple model is ease of replication, but it does not include any convolution with telescope beams. We verified the model by running the parameters Lincowski et al. (2021) used to fit an ALMA whole-planet SO_2 spectrum at 346.652 GHz (from Encrenaz et al. 2015), and found our simple code generates lines $\approx 25\%$ less deep. We also ran a verification against a prior model (Greaves et al. 2020) for the 267.537 GHz SO_2 transition, and here the simple code generated lines $\approx 15\%$ less deep. Thus if SO_2 model-lines here are $\sim 20\%$ below true depth, abundances inferred by fitting depths of observed spectra will be $\sim 25\%$ too high – an error that is likely smaller than in the observations (due to incomplete-sampling and flux-calibration issues).

Here we generate model SO_2 spectra at spectral resolutions used in the ALMA and JCMT observations. We adopt as pressure-broadening coefficient the mean-estimate of $0.18 \text{ cm}^{-1}/\text{atm}$ in Lincowski et al. (2021). The SO_2 line-strengths are from Underwood et al. (2016, via the HITRAN database), but our code now scales line-strengths for temperature as a function of altitude. This is important for modelling the “contaminating” SO_2 line, as its absorbing energy level is significantly different to that of the other observed transitions (613 K versus 93–152 K). For verification, we modelled the SO_2 $30_{9,21}-31_{8,24}/13_{3,11}-13_{2,12}$ line-pair that was observed by ALMA. The detailed radiative-transfer codes of Greaves et al. (2020), Lincowski et al. (2021) indicate this line-depth ratio is $1:40(\pm 2)$, while the simple code gives $1:31$. The simple model used here thus slightly over-estimates $\text{SO}_2/\text{J}=31$ contamination.

3. RESULTS

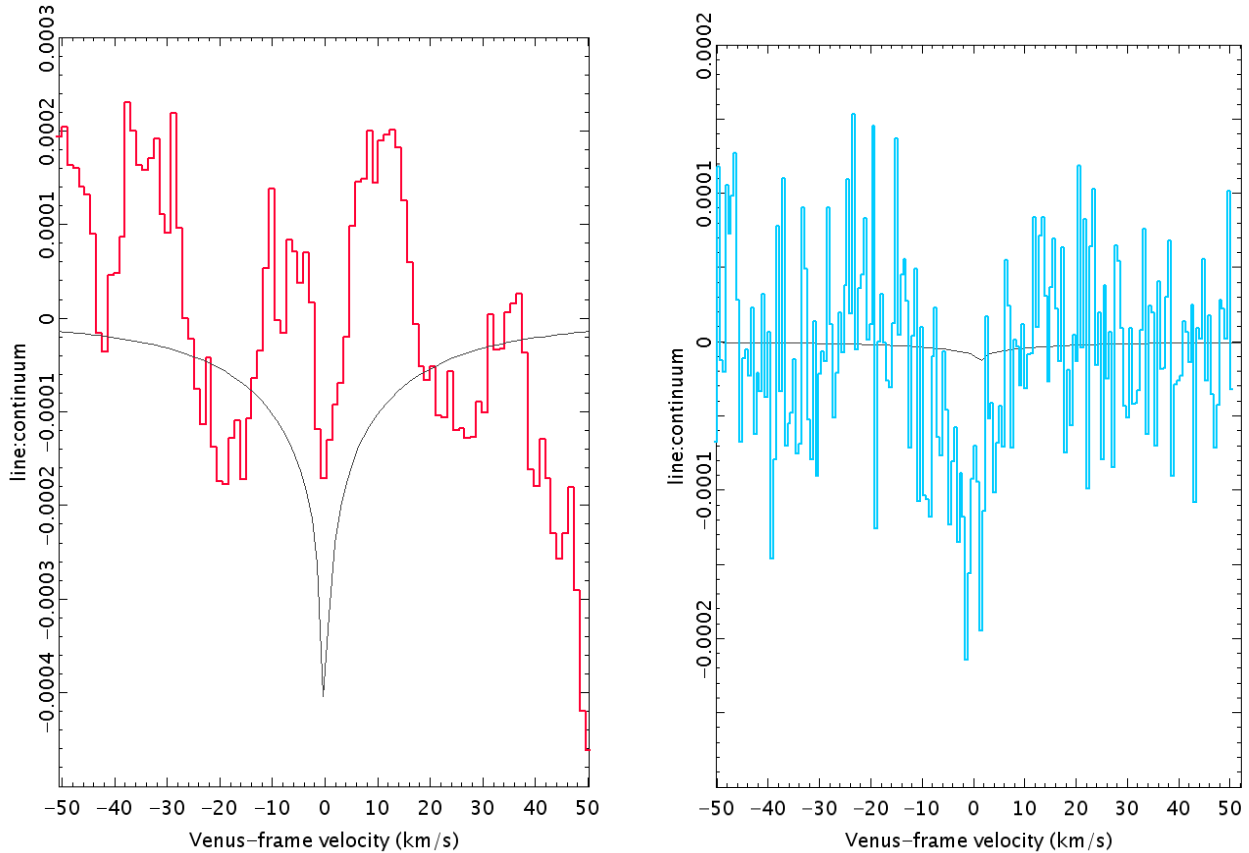
3.1 ALMA

We first verify that absorption near the PH_3 1-0 frequency is in fact detected. Figure 1 shows an optimal example (minimal residual ripple), from a planet-spanning RA,Dec “box” of 97x37 pixels (1 pixel = 0.16 arcseconds). The long axis is aligned close to the planetary equator (tilted to RA by 13°), and 49% of the planetary disc is included (no latitudes above 40°). This extracted spectrum has 7.7 sigma confidence (line-integrated over ± 6 km/s) and the line-centroid is at -0.2 ± 0.5 km/s in the Venus/ PH_3 1-0 reference-frame. This

agrees with zero as expected if the absorption is dominated by phosphine, but is 3-sigma discrepant with the alternative attribution (Lincowski et al. 2021, e.g.) to SO_2 $30_{9,21}-31_{8,24}$ absorption, which would be centred at +1.3 km/s.

Figure 1 also shows the spectrum for the same area for the SO_2 $13_{3,11}-13_{2,12}$ transition that ALMA observed simultaneously. A very weak feature is seen at Venus' velocity, but it is below the level of residual ripples. A suitable 3-sigma upper-limit model is 15 ppb of SO_2 at ≥ 80 km. We then ran the same 15 ppb model for the SO_2 $30_{9,21}-31_{8,24}$ transition. Comparing this model to the PH_3 1-0 observation, the SO_2 contamination is <10%, measured over a ± 10 km/s span (outside of which line-wings may be lost in processing – Greaves et al. 2021a).

Figure 1. Left panel, (a): ALMA wideband spectrum of SO_2 $13_{3,11}-13_{2,12}$ (red histogram) for half the planetary disc, as described in the text. The black curve is an upper-limit model, for 15 ppb of SO_2 at all altitudes ≥ 80 km, and without any baseline-fitting. Right panel, (b): spectrum at the PH_3 1-0 frequency (blue histogram) for the same planetary area. The black curve is the corresponding 15 ppb upper-limit model for the SO_2 $30_{9,21}-31_{8,24}$ transition.



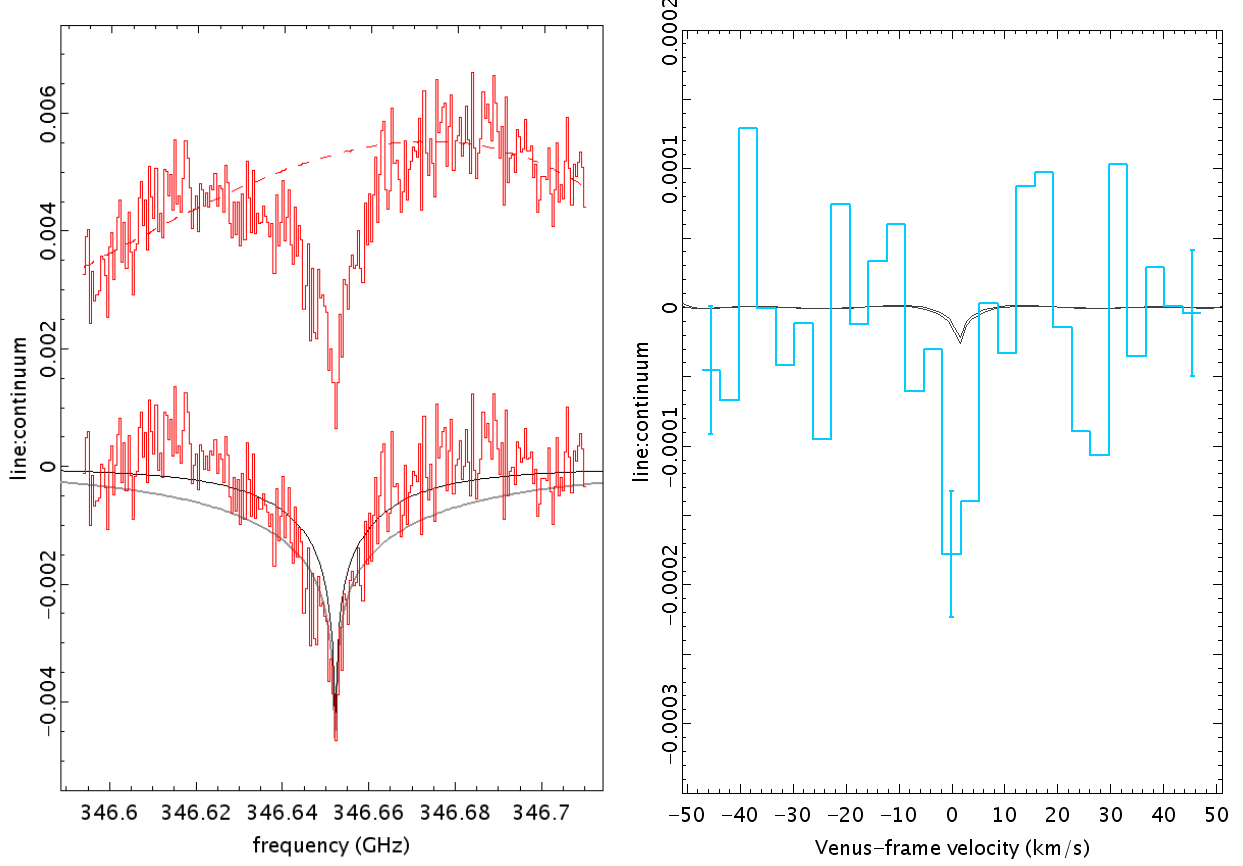
3.2 JCMT

The JCMT acquired SO_2 $19_{1,19}-18_{0,18}$ spectra on mornings 25, 17 and 6 days before the mid-point of the PH_3 run. The line-continuum ratios are similar, at -0.003 to -0.0045 at line-minimum. Figure 2 shows the SO_2 spectrum observed on 6 June 2017, closest to the PH_3 observing run. There is some spectral ripple present, which can be approximated with a low (4th) order polynomial. After subtracting this trendline from the data, we overlay two line models, one that matches the line-core well and one with a better match to the line wings. The former model is for 45 ppb of SO_2 at ≥ 75 km and the latter for 50 ppb at ≥ 80 km. The profile parameters are thus well-constrained, in spite of fit-limitations.

We then generated models for the contaminating SO_2 $30_{9,21}-31_{8,24}$ line, with these two abundance profiles. Polynomial baseline-fits were subsequently applied to these models, to match the final stage of processing applied to the observed JCMT spectra (Greaves et al. 2020). Figure 2 shows the results, demonstrating that the SO_2 line-contribution is small. The model signal, measured over ± 5 km/s, is only 6-9% of the total absorption seen in the PH_3 1-0 observation.

Given the nearly-constant SO_2 that JCMT observed in May-June 2017, it seems unlikely that the planet-wide abundance soared by an order of magnitude in the three days between the last SO_2 spectrum and the start of PH_3 observing. Large jumps in SO_2 are rare for substantial areas of Venus (Marcq et al. 2020) - an example is a 2.5-fold decline seen by HST over 5 days (Jessup et al. 2015), but only for latitudes inside $\pm 10^\circ$. We conclude that while sulphur dioxide does vary strongly on various cadences, the SO_2 and PH_3 data here are sufficiently contemporaneous that the JCMT phosphine-attributed signal can not be re-assigned to sulphur dioxide.

Figure 2. Left panel, (a): JCMT spectrum of SO_2 $19_{1,19}-18_{0,18}$ observed on June 6 2017 (upper red histogram, offset for clarity). The dashed trendline is a 4th-order polynomial fitted outside the line region. The lower histogram shows the trendline-subtracted spectrum, overlaid with two models: the darker curve is for 50 ppb of SO_2 at ≥ 80 km and the lighter (lower) curve is for 45 ppb at ≥ 75 km. Right panel, (b): the net 9-16 June 2017 JCMT spectrum of PH_3 1-0 (blue histogram, with representative 1σ errorbars), overlaid with the same two models as in (a) but for the contaminant SO_2 $30_{9,21}-31_{8,24}$ line. Observed and model spectra have had line-wings suppressed outside ± 5 km/s (see text).



4. DISCUSSION

The spectra in Figures 1 and 2 show that the absorptions proposed as PH_3 1-0 can not be re-attributed to sulphur dioxide. Contamination of the observed spectra by the high- J SO_2 transition is below 10%, with both observatories. The ALMA-detection presented here has 7.7 sigma confidence, so is ≥ 6.9 sigma even if SO_2 contamination is towards the upper limit. The JCMT spectrum with best preservation of the line-wings has 6.7 sigma confidence (Greaves et al. 2020), and is 6.2-6.3 sigma after removing contamination.

Lincowski et al. (2021) propose that high abundances of SO_2 could escape detection when larger spatial scales are filtered out in ALMA processing, and Akins et al. (2021) confirm this through simulations of a range of 2D gas-distributions. We agree with this conclusion, but emphasise that spatial filtering can not enhance SO_2 $30_{9,21}-31_{8,24}$ contamination relative to the SO_2 $13_{3,11}-13_{2,12}$ absorption. Both line-signals will be similarly filtered, as they arise from the same spatial distribution of gas and the same column of absorbing atmosphere (line-frequencies differ by <1%). Therefore, a strong

upper limit on the observed SO_2 $J=13$ line imposes a stringent upper limit on the “contaminant” $J=31$ line, such that the robustly-detected ALMA absorption at the PH_3 frequency *can not* be from SO_2 .

The only pathological variant of this argument that we can identify would involve weighting the SO_2 abundance-profile to the warmest gas-layer (where the $J=31$ level-population is higher), and making this layer particularly patchy (so $J=31$ spatial-filtering is reduced). Imagining a simple two-layer atmosphere, $J=13$ absorption could come from both a smooth cold mesosphere (temperatures down to ~ 175 K) and a warm patchy cloud deck (up to ~ 300 K). However, $J=31$ absorption (energy level >600 K) would be weighted towards warm SO_2 -rich clouds, and less of this signal would be filtered out. The result would be a stronger “contaminant” SO_2 $30_{9,21}-31_{8,24}$ line than in standard models. However, this concept severely conflicts with observations. While millimetre-wavelength absorption-spectra have some sensitivity to the clouds (Piccialli et al. 2017, Figure 7, e.g.), these observations mainly find the SO_2 that is in the mesosphere (above ~ 78 –85 km: Lincowski et al. 2021). Further, while this mesospheric SO_2 may be patchy (Encrenaz et al. 2015), lower altitudes are dominated by large-scale Hadley-cell circulation (Marcq et al. 2020), with SO_2 “plumes” rapidly smeared out by the east-west super-rotation (Encrenaz et al. 2019). A smoother SO_2 distribution at lower altitude is the opposite of what is needed for this scenario of enhanced $J=31$ absorption to work.

The net SO_2 abundances found here are typical for the gas-columns traced by millimetre-wavelength observations, for example the 4-year JCMT-monitoring programme by Sandor et al. (2010). Our 15 ppb ALMA SO_2 upper-limit from March 2019 lies in the lower-half of their abundance table, although a filtering-corrected limit could be higher (Akins et al. 2021). Our 45–50 ppb SO_2 JCMT estimate for June 2017 is by contrast in the top decile of the Sandor et al. tabulation. While both our net values are normal, SO_2 abundance-profiles using additional data tend to increase upwards (Lincowski et al. 2021). This top-weighting enabled these authors to approximately match our JCMT PH_3 -frequency spectrum using SO_2 alone. However, we can now show that their solution (Case D, Lincowski et al. 2021) is inconsistent with the JCMT SO_2 observation of Figure 2. Their SO_2 -profile peaks at ~ 400 ppb at 100 km altitude. We modelled the SO_2 $19_{1,19}-18_{0,18}$ transition using *only* a layer of 400 ppb at ≥ 100 km, and found this model spectrum already exceeds the observed line-depth (Figure 2a)

by ~50%. Including the additional sulphur dioxide molecules present from ~80–100 km would make this discrepancy far larger.

In spite of removing SO_2 contamination, it is still problematic to infer abundances, assuming that the absorber is phosphine (and not some as-yet uncatalogued molecule). Villanueva et al. (2021) argue that the narrow observed lines suggest PH_3 would have to be solely mesospheric – increasing the required abundance as less of the total gas-column is occupied by molecules. We agree that the preliminary constant-abundance profile of Greaves et al. (2020) could not in fact match the observed spectra – see discussion in Greaves et al. (2021a). However, the cloud-level contribution is still to be assessed, given the characteristic line-wings are heavily suppressed in necessary processing. A purely mesospheric location is agreed to be problematic because PH_3 molecules should rapidly photodissociate, unless upwards diffusion is much faster than expected (Greaves et al. 2021a).

Here we highlight that, although abundances remain unknown, the line-depths retrieved by JCMT and ALMA are now found to be similar. After subtracting contamination and adopting uniform ≈ 3.5 km/s spectral binning, the line-minimum for JCMT is $-1.6\text{e-}4$ to $-2.2\text{e-}4$ (for alternate baselining-strategies of Greaves et al. 2020) versus $-1.1\text{e-}4$ to $-1.2\text{e-}4$ for ALMA (for zero to 3-sigma contamination-levels). The variation seen is thus ~25% around -0.015% of the continuum. The true ALMA line-depth is uncertain due to the unknown effects of spatial filtering; in particular, the absorption would be less deep using a Venus-model continuum rather than the filtered continuum (Akins et al. 2021, Greaves et al. 2021a). However, as ALMA and JCMT both sampled large areas of Venus (respectively: $\sim 1/3$, limb-weighted and $\sim 1/2$, centre-weighted), the similarity in absorption suggests that phosphine-attributed abundances were broadly comparable in 2017 and 2019.

Acknowledgements: JCMT data newly presented here were obtained under program id M17AP081 and retrieved from the archive hosted at CADC. We thank the PI, Hideo Sagawa, for valuable consultations about interpretation of these observations. The James Clerk Maxwell Telescope is operated by the East Asian Observatory on behalf of The National Astronomical Observatory of Japan; Academia Sinica Institute of Astronomy and Astrophysics; the Korea Astronomy and Space Science Institute; Center for Astronomical Mega-Science (as well as

the National Key R&D Program of China with No. 2017YFA0402700). Additional funding support is provided by the Science and Technology Facilities Council of the United Kingdom and participating universities and organizations in the United Kingdom and Canada. This research used the facilities of the Canadian Astronomy Data Centre operated by the National Research Council of Canada with the support of the Canadian Space Agency. SMURF and SPLAT software were provided via <http://www.starlink.ac.uk/docs/starlinksummary.html>, the home of the UK's Starlink Project.

References:

Akins, A.B., Lincowski, A.P., Meadows, V.S. & Steffes, P.G. 2021, *ApJ*, 907, L27

Bains, W., Petkowski, J.J., Seager, S., et al. 2021, *AsBio*, doi.org/10.1089/ast.2020.2352

Encrenaz, T., Greathouse, T.K., Marcq, E., et al. 2020, *A&A*, 639, 69

Encrenaz, T., Greathouse, T.K., Marcq, E., et al. 2019, *A&A*, 623, A70

Encrenaz, T., Moreno, R., Moullet, A., Lellouch, E. & Fouchet, T. 2015, *P&SS*, 113, 275

Greaves, J.S., Richards, A.M.S., Bains, W., et al. 2020, *NatAs*, doi.org/10.1038/s41550-020-1174-4

Greaves, J.S., Richards, A.M.S., Bains, W., et al. 2021a, *NatAs*, 5, 636

Greaves, J.S., Bains, W., Petkowski, J.J., et al. 2021b, *NatAs*, 5, 726

Hallsworth, J.E., Koop, T., Dalaa, T.D., et al. 2021 *NatAs*, 5, 665

Jessup, K.L., Marcq, E., Mill, F., et al., 2015, *Icar*, 258, 309

Lincowski, A.P., Meadows, V.S., Crisp, D., et al. 2021, *ApJ*, 908, L44

Marcq, E., Jessup, K.L., Baggio, L., et al. 2020, *Icar*, 335, 113368

Mogul, R., Limaye, S.S., Way, M.J., et al. 2021, *GeoRL*, 48, 91327

Piccialli, A., Moreno, R., Encrenaz, T., et al. 2017, *A&A* 606, 53

Sandor, B.J., Clancy, R.T., Moriarty-Schieven, G., Mills, F.P. 2010, *Icarus*, 208, 49

Seager, S., Petkowski, J.J., Gao, P., et al. 2021, *AsBio*, doi.org/10.1089/ast.2020.2244

Snellen, I.A.G., Guzman-Ramirez, L., Hogerheijde, M.R., Hygate, A.P.S. & van der Tak, F.F.S. 2020, *A&A*, 644, L2

Thompson, M.A. 2021, *MNRAS*, 501, L18

Trompet, L., Robert, S., Mahieux, A., et al. 2021, *A&A*, 645, L4

Underwood, D.S., Tennyson, J., Yurchenko, S.N., et al., 2016, *MNRAS*, 459, 3890

Villanueva, G., Cordiner, M., Irwin, P., et al. 2021, *NatAs*, 5, 631

APPENDIX: LINE PROFILE MODEL

We develop a semi-analytical one-dimensional model for the line profile, starting at the surface of Venus, height $z = 0$ km, and moving up in height increments based on the same temperature profile used by Greaves et al. (2021a), with the top of the atmosphere at 115 km.

We track the intensity as a function of height (z , km) and frequency (ν , Hz), with a line center at ν_0 (Hz):

$$I = I(\nu, \nu_0, z), \quad (1)$$

We set $I(\nu, \nu_0, 0)$ equal to unity over all frequencies. For each step, Δz (km), from 0 km to 115 km, we update:

$$I(\nu, \nu_0, z + \Delta z) = I(\nu, \nu_0, z) e^{-\tau(z, z + \Delta z)} + \frac{B_\nu(z)}{B_\nu(0)} e^{-\tau(z, z + \Delta z)}, \quad (2)$$

where τ is the optical depth between z and $z + \Delta z$, given by:

$$\tau(z, z + \Delta z) = f_V(\nu, \nu_0, z) S_{\nu_0}^*(z) \Delta z. \quad (3)$$

$f_V(\nu, \nu_0, z)$ is the Voigt profile, and depends on the gas temperature T (K) and pressure p (bar), both functions of height, z , and on the pressure-broadening coefficient γ ($\text{cm}^{-1} \text{ atm}^{-1}$). The line-strength, $S_{\nu_0}^*$ ($\text{cm}^{-1} \text{ s}^{-1}$) is:

$$S_{\nu_0}^*(z) = c n(z) e^{E_J/T_0} e^{-E_J/T(z)} S_{\nu_0}, \quad (4)$$

where $c = 2.9979 \times 10^{10}$ cm/s is the speed of light, $n(z)$ (cm^{-3}) is the number density of the absorbing species, E_J (K) is the value of the lower energy level, T (K) is the temperature and S_{ν_0} $\text{cm}^{-1}/(\text{molecules cm}^{-2})$ is the line strength at $T_0 = 300$ K. The reason for the two Boltzmann terms is to scale S_{ν_0} to different temperatures. We assume that the atmospheric gas at each height is in local thermodynamic equilibrium and therefore the population of the lower level is proportional to $e^{-E_J/T}$. We also assume that the gas in the experiment used to measure S_{ν_0} at T_0 is also in local thermodynamic equilibrium, and therefore is proportional to e^{-E_J/T_0} . We can achieve the line strength appropriate for T by dividing the former Boltzmann factor by the latter.

Finally $B_\nu(z)$ is the spectral radiance given by Planck's law:

$$B_\nu(z) = \frac{2h\nu^3}{c^2} \frac{1}{e^{h\nu/(kT)} - 1}, \quad (5)$$

where $h = 6.62607 \times 10^{-27}$ erg s is Planck's constant and $k = 1.38065 \times 10^{-16}$ erg/K is Boltzmann's constant.

This one-dimensional model accounts for absorption and thermal emission, but does not treat scattering. Scattering will increase the path length traversed and is therefore expected to strengthen the absorption features. Unless scattering is steeply dependent on frequency, this effect will be approximately the same for each line, and so the ratio of line strengths will not be affected.

This program calculates a single line profile and is written in Python3. The code to model the SO_2 $13_{3,11}-13_{2,12}$ transition can be found at <http://www.mrao.cam.ac.uk/~pbr27/J13.py>.